Rare Metal Materials and Engineering
Volume 50, Issue 9, September 2021
Available online at www.rmme.ac.cn

Science Press

Cite this article as: Wang Miao, Yang Shuangping, Liu Haijin, et al. Research Progress and Prospect of Strengthening and Toughening of Molybdenum Alloys[J]. Rare Metal Materials and Engineering, 2021, 50(09): 3158-3168.

REVIEW

Research Progress and Prospect of Strengthening and Toughening of Molybdenum Alloys

Wang Miao[1,2], Yang Shuangping[1], Liu Haijin[1], Yang Xin[1], Wang Lidong[1]

[1] School of Metallurgical Engineering, Xi'an University of Architecture and Technology, Xi'an 710055, China; [2] Research Center of Metallurgical Engineering and Technology of Shaanxi Province, Xi'an 710055, China

Abstract: The molybdenum alloy has received more and more attention in various industrial fields, but its extensive applications are restricted due to the degradation of its creep resistance, strength, and oxidation resistance at high temperature, and the lack of effective mass production methods. This research analyzes the brittleness source of pure molybdenum, and reveals that the improvement of extrinsic brittleness and innovation of preparation process are the key directions of research and development of molybdenum alloys. The methods applied for strengthening and toughening of molybdenum alloys are reviewed, and the research and application status of typical molybdenum alloys are listed. In addition, in consideration of the existing problems, the research direction of high temperature molybdenum alloys is summarized.

Key words: molybdenum alloy; strengthening and toughening; powder metallurgy technique; solid solution strengthening; second phase dispersion strengthening; alloying

Molybdenum alloy has broad application prospects in aerospace, high temperature heating devices, forging molds, and other fields, but its application and deep processing performance are restricted due to the structural feature weakness and high temperature anti-oxidation properties. Alloying has been accepted and adopted by numerous scholars for reducing the grain boundary embrittlement[1].

At present, various types of Mo alloys, such as titanium-zirconium-molybdenum (TZM), molybdenum-hafnium-carbon (MHC), oxide dispersion strengthening (ODS) -Mo, and La-TZM, have been widely researched. Lang et al[2] prepared MHC alloy via powder metallurgy (PM) route, which is hardened by nanoscale HfC precipitation. Tan et al[3] fabricated 10wt% MoAlB reinforced Mo-12Si-8.5B alloy by spark plasma sintering. The composite shows an enhanced strength, hardness, and a remarkably improved wear resistance. Hu et al[4] investigated the secondary phase formation in La-TZM alloy and found that La doping improves the temperature sensitivity and mechanical properties. Hu et al[5] indicated that nano-TiC and ZrC decrease the size of micron secondary phase of La-TZM alloy by 26.7% and increase the yield strength by 27% to reach 1239 MPa. Liu et al[6] proposed the idea of nano-doping strengthening and toughening with nanoscale rare earth oxide particles uniformly dispersed in the fine-grained Mo matrix based on the physical quantitative analysis model. The yield strength of the prepared nanoscale Mo alloy reaches 800 MPa with elongation of 40%. Fu et al[7] conducted a comparative study on the mechanical properties of different types of nanoscale rare-earth-oxide-doped Mo alloys, indicating that CeO_2 exhibits better performance.

Based on the existing research results, the emphasis of this research is the detailed introduction of brittleness source, and existing strengthening and toughening forms. The preparation methods and future development direction of Mo alloys are also summarized.

1 Source of Brittleness

Rolled Mo alloy exhibits high strength and toughness, and its tensile strength ranges from 600 MPa to 700 MPa.

Received date: September 07, 2020
Foundation item: Shaanxi Science and Technology Coordination Innovation Project Plan (2015KTZDGY09-01); Shaanxi Provincial Department of Education Special Scientific Research Project (17JK0439)
Corresponding author: Yang Shuangping, Ph. D., Professor, School of Metallurgical Engineering, Xi'an University of Architecture and Technology, Xi'an 710055, P. R. China, Tel: 0086-29-82202923, E-mail: yang_sping@163.com

However, after melting and resolidification treatments, Mo grain boundary is subjected to significant brittleness and the strength of treated alloy is only 20%~30% of the strength of rolled Mo[8]. The causes of brittleness are intrinsic structure and extrinsic brittleness.

Firstly, the outermost and outer electronic layers of Mo atoms are half-full ($4d^5 5s^1$). The $4d^5$ layer is asymmetrically distributed, exhibiting covalent bond properties; while the $5s^1$ layer is spherically symmetrical distributed, presenting the metallic bond properties. Changes in external conditions cause different plasticity and brittleness characteristics. Plastic deformation and brittle fracture occur when metal bonds and covalent bonds dominate, respectively. The outer electrons of Mo atoms gradually change from metal bonds to covalent bonds as the temperature decreases. If the temperature drops to below the ductile-brittle transition temperature (DBTT), the covalent bond characteristics are obvious, the lattice resistance increases sharply, and the decrease of movable dislocations leads to planar slip, resulting in stress concentration at grain boundary and a tendency of brittle fracture along the crystal[9]. In addition, the body centered cubic (bcc) structure of Mo is characterized by a few independent slip systems in cell. Therefore, the poor coordinating deformation ability between grains can lead to fracture when stress is generated at grain boundary and plastic deformation occurs at a lower temperature[10].

The second source is extrinsic brittleness caused by impurity element. Small amounts of solid solution of O, C, N, and other elements are inevitable in the fabrication process. These elements are precipitated as oxides, nitrides, etc., segregated at grain boundaries, sub-grain boundaries, and dislocations, which decreases the grain boundary strength, hinders the dislocation motion, promotes the crack formation, and eventually results in typical room temperature brittleness as a combined negative effect[11-13]. If the alloy contains elements such as Fe, P, Al, and S, which easily form related oxides, the mechanical properties are seriously affected.

It can be concluded from the above analyses that Mo has intrinsic properties of ductile-brittle transition and low-temperature brittleness caused by bcc structure, and it is sensitive to segregation of interstitial atoms, such as oxygen and nitrogen at grain boundaries inherited from preparation process. Since intrinsic brittleness can hardly change, the comprehensive optimization of extrinsic brittleness and preparation process is the main direction of research and development of Mo alloys. Firstly, the addition of some subgroup elements, such as Co, Ni, and Re, can change the electron configuration at the s orbit and d orbit in the outermost layer to improve grain boundary strength. Secondly, various reinforced elements, such as Ti, Zr, Hf, and C, can be adopted to form intermetallic compounds in Mo alloy. Therefore, the oxygen content decreases, the second phase particles are pinned at grain boundary, and dislocation further increases the strength. Thirdly, the innovation of preparation process is effective to produce low oxygen and nitrogen for Mo alloy to control the segregation in interstitial impurities.

2 Fabrication Process

Most Mo and its alloy billets are prepared by PM. PM process can obtain finer grain structure and more homogeneous structure properties, and control the composition, density, and microstructure. But products after PM are usually semi-finished and must be machined because of production process constraints on geometric flexibility. Thus, the structure deformation is severe after forging, rolling, drawing, swaging, or other treatments. Furthermore, the thermodynamically unstable state caused by PM is prone to relaxation in high temperature application, and recrystallization occurs at 900 °C. The recrystallized Mo and its alloy are prone to brittle fracture which leads to the decrease of performance. The recrystallization completed at 1200 °C may cause formation of equiaxed crystal structure which easily results in grain boundary sliding and deformation, and embrittlement occurs at room temperature, thus further restricting the application. The absorption of oxygen during PM and machining process is also inevitable.

The distribution of second phase particles depends on the doping method during powder preparation, including solid-solid (SS) mixing, liquid-solid (LS) spray mixing, and liquid-liquid (LL) mixing. Cheng et al[14] studied the mechanical property and microstructure of ODS-Mo alloy prepared by SS and LS mixing and pure Mo prepared by PM. As shown in Table 1, the yield strength and tensile strength are obviously improved by rare earth oxide doping, and LS-Mo alloy exhibits better strength than SS-Mo does.

The comparison schematic diagrams of LS and LL doping are shown in Fig. 1[15]. For LS-Mo in Fig. 1a, Mo and La initially exist as MoO_3 powder and La^{3+} ions in the solution, respectively. Mo powder and La_2O_3 particles are obtained through liquid-solid conversion, and the small La_2O_3 particles are regarded as the second phase attached to Mo through physical bonding. For LL-Mo in Fig. 1b, Mo is uniformly distributed in the liquid solution, the reaction begins since the precipitation of $NH_4La(Mo_2O_7)_2$, and then $(NH_4)_2Mo_2O_7$ is induced to nucleate unevenly on $NH_4La(Mo_2O_7)_2$, forming a core-shell structure of La_2O_3 inside the Mo grains, preventing the aggregation and maintaining the La_2O_3 particles at nanocale. By adjusting the composition and distribution of La_2O_3 inside the grain and at the grain boundary, the fine second phase hinders the growth of grains during sintering, thereby reducing the tendency of intergranular fracture. Meanwhile, the fine and dispersed second phase can effectively accumulate dislocations during tensile test, thereby

Table 1 Uniaxial tensile test results of pure Mo, SS-Mo, and LS-Mo alloys[14]

Alloy	Yield strength/MPa	Tensile strength/MPa	Elongation/%	Area reduction/%
Pure Mo	448	474	44	8
SS-Mo	532	552	42	72
LS-Mo	665	699	45	66

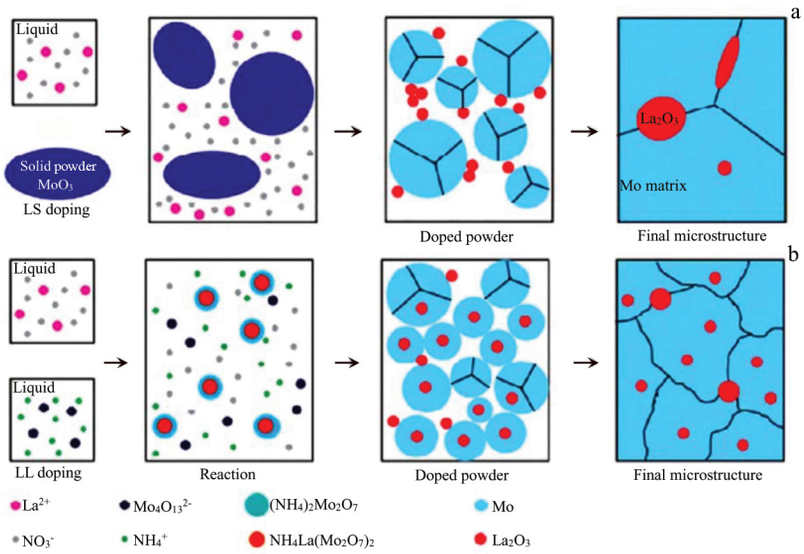

Fig.1 Schematic diagram of LS doping (a) and LL doping (b)[15]

improving the work hardening ability.

Kaserer et al[16] adopted laser powder-bed fusion (LPBF) and pre-alloyed spherical TZM powder after sieving with mesh size of 63 μm to produce highly complex near-net-shape TZM alloy parts. Results show that Mo_2C is precipitated in the grain, and the impurity oxygen forms ZrO_2 and is precipitated in the grain of ternary molybdenum-titanium carbide. Segregation of oxygen at grain boundaries cannot be detected, indicating that grain boundaries are effectively purified and alloying elements can suppress the segregation of oxygen at grain boundaries; as a result the crack-free samples with the density of 99.7% ard obtained.

3 Typical Molybdenum Alloy and Strengthening Forms

The commonly adopted strengthening methods include solid solution strengthening, second phase dispersion strengthening, bubble strengthening, and composite strengthening. Application of one or more methods can improve the mechanical and comprehensive properties for application under complex conditions.

3.1 Solid solution strengthened molybdenum alloys

The first type is to add a small amount of single alloying element (Ti, Zr, Hf, Co) into Mo alloys to form a dispersion, such as (Mo, Ti)$_x$O$_y$ and (Mo, Hf)$_x$O$_y$. Typical alloys are Mo-0.5Ti, Mo-0.5Zr, etc. In 1960s, Eck et al[17] firstly studied the influence of alloying element on strength at room temperature. The strengthening effect of Zr is the most remarkable, followed by that of Hf, Ti, and Nb.

Fan et al[18] prepared Mo-Zr and Mo-Ti alloys by PM method, indicating that Zr and TiH_2 powders show more positive effect on tensile strength than ZrH_2 and Ti do, because the continuous cold welding and crushing during ball milling process facilitates the diffusion of Zr into Mo matrix for solid solution. TiH_2 is difficult to dissolve but easy to decompose into smaller particles during ball milling, and it is uniformly distributed in the matrix. The solid solution is obtained after the decomposition of TiH_2 during sintering. Only a small amount of Zr enters the Mo matrix while the rest are combined with O due to the relatively strong affinity between Zr and O, resulting in the solid solution strengthening effect by the distribution of O inside the grain and at the grain boundary, as indicated by the scanning electron microscope (SEM) image in Fig.2a; therefore the intrinsic brittleness and tensile strength are effectively improved. Ti produced by decomposition of TiH_2 is dissolved into Mo matrix to form a solid solution, leaving only a small amount of oxide distributed at grain boundary (Fig.2b).

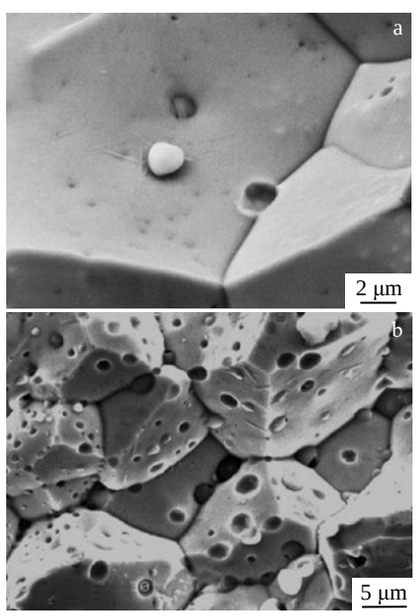

Fig.2 SEM images of Mo-0.1Zr (a) and Mo-0.8Ti (b) alloys[18]

Zhang[19] observed the changes in the microstructure of the electron beam welded TZM alloy joints through transmission electron microscope (TEM) and selected area electron diffraction (SAED) patterns, and found the similar conclusion, i. e., most Zr and Ti are combined with intracrystalline impurity element O to form oxide, instead of dissolving into Mo matrix[18].

The second type is to use a large amount of solid solution to strengthen Mo alloy and the typical alloys are Mo-W and Mo-Re. Since Re has close-packed hexagonal (hcp) structure and the alloy has bcc structure, the addition of a certain amount of Re can effectively reduce the yield strength of molybdenum, i.e., Re softening effect[20]. Fig. 3 shows the mechanical properties of Mo-41Re, Mo-5Re, and pure Mo. When annealing temperature is raised from room temperature to 2200 °C, Mo-41Re shows excellent strength and ductility. Sturm et al[21] proposed that Re reduces the directionality of matrix metal bond and the energy of stacking defect, and increases the shear modulus and solubility of interstitial impurities, thereby improving plasticity. Mo-Re alloys also have neutron radiation and corrosion resistance. However, the cost of Re restricts the wide application of Mo-Re alloys.

Both Mo and W have bcc structure, and W can form continuous solid solution in Mo matrix. The forging plastic deformation resistance increases, especially when W addition is above 20%. Ohser-Wiedemann et al[22] prepared Mo-W powder by high-energy ball milling and the high defect density generated inside the crystal grains was found, resulting in the interdiffusion between Mo and W during sintering process and an acceleration of solid solution effect, as indicated by the SEM-backscattered electron (BSE) images of flake microstructure inside the crystal grains (Fig.4). As the milling time increases, the flake structure becomes finer, enhancing the mutual diffusion.

Wang et al[23] found that the tensile strength and elongation of Mo-30W prepared by PM process are 170 MPa at 1600 °C and 10%, respectively, the former of which is higher than that of pure Mo (142 MPa at 1200 °C). This is mainly due to the solid solution strengthening effect by W and deformation strengthening. After forging and deformation, the crystal grains are elongated and deformed to from a small equiaxed shape, and gradually become fibrous structure. The bonding force between the grains is enhanced, and the sensitivity to cracks greatly reduces. Thus the material can withstand larger deformation before breaking.

Ohser-Wiedemann et al[22] proposed the interaction theory of dislocations and impurity atoms for explaining the strengthening mechanism. When a small number of solid solution atoms are formed, the atomic distribution is in the largest dislocation accumulation region in the matrix. Due to the elastic stress field around the impurity atoms and dislocations, the interaction occurs along the direction of reducing the total elastic stress. The imperfections of the lattice make internal energy of alloy lower than that of pure metals. Therefore, due to the addition of a small amount solid solution element, the unsolid solution components are likely combined with oxygen to form oxides and reduce the tensile strength of the alloy, resulting in the increase of brittleness. So, the addition of solid solution elements should be strictly controlled. The addition of a large amount of solid solution Re and W can significantly improve the alloy properties, but the price of Mo-Re alloys and the poor processing performance of Mo-W alloys restrict the wide application.

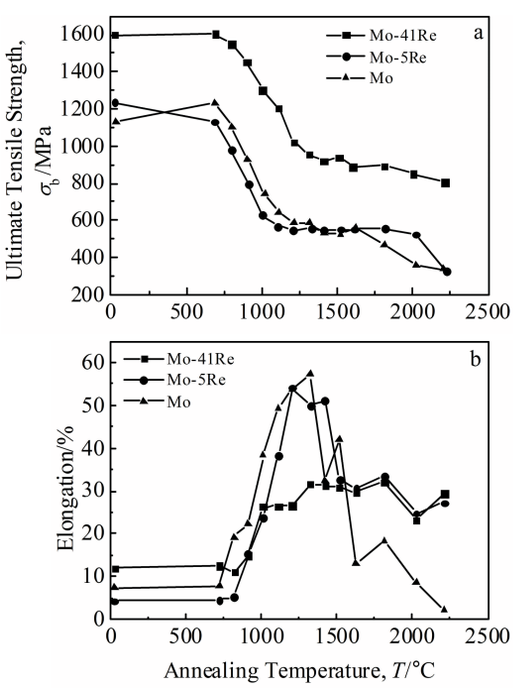

Fig.3 Effect of annealing temperature on ultimate tensile strength (a) and elongation (b) of Mo-Re wire and pure Mo sheet at room temperature[20]

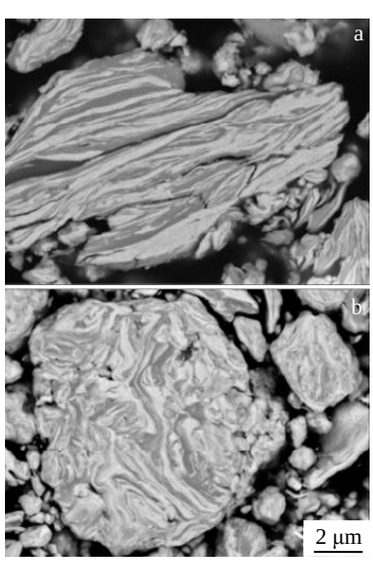

Fig.4 SEM-BSE images of flake microstructure of Mo-50W composites after high-energy ball milling for 20 h (a) and 40 h (b)[22]

3.2 Second phase dispersion reinforced molybdenum alloys

Carbide, rare earth oxide, and other oxides can absorb energy when material fractures, and they are used as second phase dispersion particles. A transformed Hall-Petch formula can describe the contribution of yield strength, as follows[15]:

$$\sigma_s=\sigma_i+Kd^{-1/2}+\sigma_{intra}+\sigma_{inter} \quad (1)$$

where, σ_s is the yield strength, σ_i is the strength of the metal matrix before deformation, $Kd^{-1/2}$ is refined grain contribution strength, K is slope of the Hall-Petch relationship, d is grain size, σ_{intra} is the intensity contributed by grains, and σ_{inter} is the intensity contributed by grains between grains.

3.2.1 Carbide dispersion strengthening alloy

Carbide dispersion strengthening alloy relies on the formation of diffused fine carbides of high-melting point through the reaction between carbon and active elements, such as Ti, Zr, and Hf. Kitsunai[24,25] and Kmishiha[26] et al prepared Mo-0.2wt% TiC alloy by mechanical alloying and hot isostatic pressing. The dispersed TiC particles can prevent the migration of grain boundaries in matrix Mo, refine the Mo grains, restrict the interfacial slip between TiC and matrix, and effectively increase recrystallization temperature. The comparison of TiC, HfC, ZrC, and TaC[24-26] indicates that the best grain refining effect is obtained by ZrC and HfC, whose average grain size is reduced from 40 μm to 4~5 μm after heating at 2000 °C.

Pöhl[27], Lang[2,28], and Siller[29] prepared MHC alloys with 0.65at% Hf and 0.65at% C by PM process. The formation of HfC improves the performance, which is influenced by the annealing temperature, as shown in Fig. 5. It can be observed that HfO_2, Mo_2C, and plate-like HfC exist in the microstructure, as shown in Fig. 5a and 5b. Although HfO_2 particles and Mo_2C layers still exist in the microstructures, as shown in Fig. 5c~5f, a change in the HfC quantity can be observed. By increasing the annealing temperature, HfC phase becomes less in Fig. 5c and 5d, and nearly vanishes with few scattered particles, as shown in Fig.5e and 5f.

Yang et al[30] studied the effect of HfC addition on the high-temperature plasma ablation properties of Mo-W alloys. Results indicate that because of the high melting point and larger thermal expansion coefficient of HfC, the ablation resistance can be significantly improved by the formation of HfO_2 with low thermal conductivity and good fluidity covering the surface of matrix.

The carbon nanotubes (CNTs) were used to in-situ synthesize TiC/Mo-based composites via LPBF method[31]. The functionalized CNTs were dispersed with MoTiAl powders under electrostatic attraction by hetero agglomeration. During LPBF, individual CNTs react with Ti elements and are completely transformed into monocrystalline TiC. Since the in-situ TiC does not retain the tube shape of CNTs, it can be concluded that nano-TiC is preferentially formed between dangling carbon atoms and Ti elements and then grows during the interdiffusion process. Notably, the TiC/MoTiAl interface is extremely tight and clean without interfacial impurities or nano-cracks. This is mainly attributed to the similar coefficients of thermal expansion between TiC and Mo. The investigation of influence of in-situ formed TiC on the crystallization behavior of MoTiAl matrix shows that TiC reinforcements connect to the matrix and are homogeneously dispersed, leading to morphological evolution of MoTiAl matrix from nearly columnar to fine equiaxed grains, thereby improving the mechanical performance. Besides, the electron back-scattered diffraction (EBSD) phase mappings suggest that the quantity of TiC formation in this composite is approximately 11.1vol%, which is similar to the

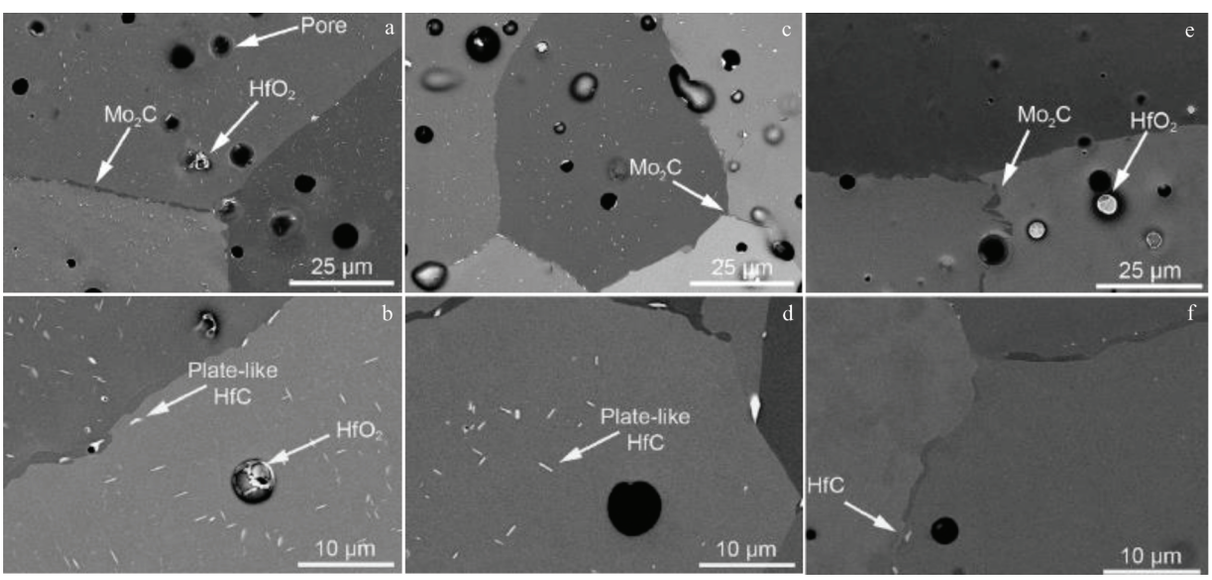

Fig.5 SEM-BSE images of microstructures of electrolytically polished MHC alloys under different annealing conditions: (a, b) 1600 °C/20 h, (c, d) 2000 °C/5 h, and (e, f) 2300 °C/5 h[27]

expected value under the assumption that CNTs are completely reacted with TiC structures.

Therefore, the addition of an appropriate amount of alloying elements to form fine and uniformly dispersed carbide second phases to hinder the movement of dislocations can significantly improve the strength and ablation properties.

3.2.2 Oxide dispersion strengthening alloy

(1) Rare earth ODS alloy

Zhang et al[32] studied the strengthening mechanism of La_2O_3 doped Mo alloys. It is believed that there are multi-scale La_2O_3 particles after quantitative analysis of the grain size. The contribution of La_2O_3 particle to grain refinement is 31~103 MPa, and the contribution intensity is 88~124 MPa. In addition, the volume fraction of fine particles is much larger than that of coarse particles and the contribution of fine particles to strength is significant.

For metal materials containing second phase particles, the mismatch between second phase particles and matrix in terms of elastic modulus and deformability is inevitable. Therefore, in the process of deformation, local stress/strain concentration is inevitable to occur at second phase particles, causing the formation of cracks and ultimately leading to material failure. As the second phase particle size increases, it is more difficult to coordinate the deformation between the particles and the matrix, thereby easily causing micro-cracks and reducing the ductility. As shown in Fig. 6, the rare earth oxide particles are mainly located on the grain boundary, where the stress/strain is concentrated during deformation. Thus, micro-cracks are often initiated at the grain boundary and cause intergranular cracking (Fig. 6b). In addition, the large size of rare earth particles and high stress/strain concentration can also lead to particle/matrix interface de-adhesion (Fig. 6c) and particle fracture (Fig.6d), further accelerating the failure process.

Feng et al[33] exploited the nanoparticle spray doping technique and investigated the influences on mechanical properties and microstructure of ODS-Mo. La_2O_3 soliquoid with size of 30~50 nm is uniformly sprayed into double-cone doping tank containing MoO_2 powders and rotating at constant velocity under the condition of temperature of 333~336 K and compressed air of 0.4~0.8 MPa. The soliquoid is continuously stirred by the electromagnetic stirrer to prevent the precipitation and aggregation of dopants particles. At room temperature, the yield strength and tensile strength of Mo-La wires fabricated by the nanoparticle spray doping technique are about 50% higher than those of the corresponding Mo-La alloys fabricated by LS mixing. TEM observations (Fig. 7) reveal that the number, size, and distribution of second phase particles of Mo-La alloys prepared by the two methods are quite different.

The second phase particles are rarely observed in the Mo grains and dislocation (Fig. 7a), and the La_2O_3 particles prepared by LS process are micron level. A large number of second phase particles with nanometer scale are distributed homogeneously in the intragranular and intergranular Mo substrates by nanoparticle spray doped technique (Fig. 7c and 7d), which plays an important role in the effect of dispersion strengthening.

Fu et al[7] found that CeO_2 particles deform together with Mo matrix due to the coherent relationship. Therefore, the strengthening mechanism is the combination effect of coherent toughening and dispersion strengthening, resulting in the excellent room temperature and high temperature mechanical properties of nano-CeO_2 doped Mo alloy, compared with those of nano-Y_2O_3 and La_2O_3 doped alloys, as shown in Fig. 8. The La_2O_3 particles are about 30 nm in size, evenly distributed in the crystal grains and at grain

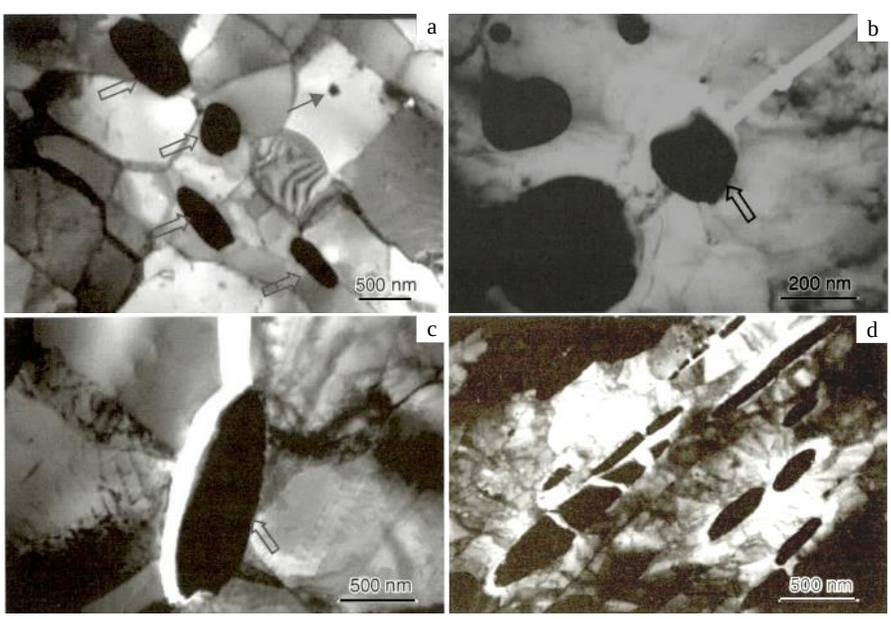

Fig.6 Typical TEM images of ODS Mo alloys: (a) distribution of second phase particles; (b~d) micro-cracks initiated at second phase particles[32]

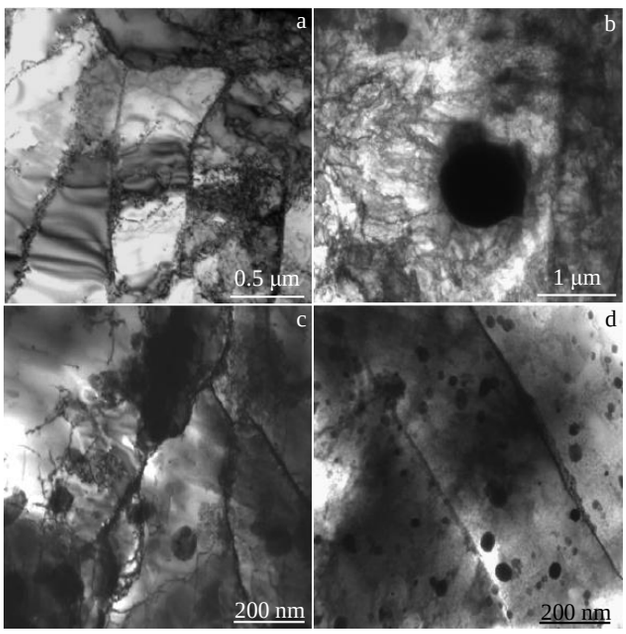

Fig.7 TEM images of microstructures of Mo-0.3La alloys prepared by LS spray doping (a, b) and nanoparticle spray doping (c, d) processes[33]

boundaries, and are not deformed at all, mainly playing a role of dispersion strengthening. The particles size of Y_2O_3 is relatively large, 60~80 nm, and Y_2O_3 is mostly segregated at the grain boundaries without significant deformation, which results in a relatively weak toughening effect.

The strengthening and toughening mechanisms of ODS Mo alloy has attracted researchers' attention and current researches mainly focus on fine-grain strengthening, second-phase particle dispersion strengthening, and Orowan dislocation strengthening.

(2) Other oxide dispersion and chemical compound strengthening alloys

The addition of Al_2O_3 and ZrO_2 ceramic phases into Mo matrix has gradually become a research hotspot.

Hu et al[34] prepared Al_2O_3/Mo composites with a doping content of 1.0wt% through the hydrothermal synthesis-low temperature calcination-reduction-sintering route. After low temperature calcination, MoO_3 of orthogonal structure and intermediate $Al_2(MoO_4)_3$ phase are formed. After hydrogen reductions, the second phase is completely transformed into α-Al_2O_3 and dispersedly distributed in the Mo matrix. This is consistent with the results in Ref. [35, 36]. During high temperature sintering, the nanosized α-Al_2O_3 particles agglomerate to form micron-sized α-Al_2O_3 because of interface atomic diffusion. Because the micron-sized α-Al_2O_3 grains are formed from the orderly grown α-Al_2O_3 nanoparticles, the fine structure of α-Al_2O_3 grain is characterized by the orderly combination of several nano grains. The Al_2O_3 particles can refine the Mo grains[37] and remarkably increase the microhardness, eleastic modulus, and yield strength. The maximum yield strength of alloy containing 1.28vol% Al_2O_3 increases by 61.07%~90.2%, compared with that of pure Mo after annealing at 1000~1300 °C[38].

TEM observation of Al_2O_3/Mo composite in Fig.9 indicates that two phases are well fitted with two sets of SAED patterns which belong to Al_2O_3 and Mo phase, proving that there is no chemical reaction after high temperature sintering[35]. The crystal lattice at the interface (the area between the red lines in Fig. 9c) intersects and overlaps with each other, proving that the two phases are firmly bonded with the interface width of 4~5 nm. The close combination of Mo matrix and the second phase particles can form a dense structure by sintering process and block the effect on the diffusion of Mo atoms by the dispersed second phase particles, resulting in fine Mo matrix grains[35,36].

Cui et al[39] prepared ZrO_2/Mo alloy by hydrothermal method and PM process. ZrO_2 particles are located at grain boundaries and inside the grains, and finer particles are distributed inside Mo grains while slightly larger particles are distributed at grain boundaries. By the pinning effect of the second phase, recrystallization process is delayed and high temperature mechanical properties are enhanced.

Microstructure after compressing test is shown in Fig. 10. There is a second particle, as shown in the middle of Fig.10a, surrounded by many dislocations, as indicated by the arrows. The detachment of the second phase particles from the matrix can also be observed. The number of dislocations is increased with increasing the deformation. When the number of dislocations reaches a certain value, the second phase particles are separated from the matrix, which hinders the dislocation

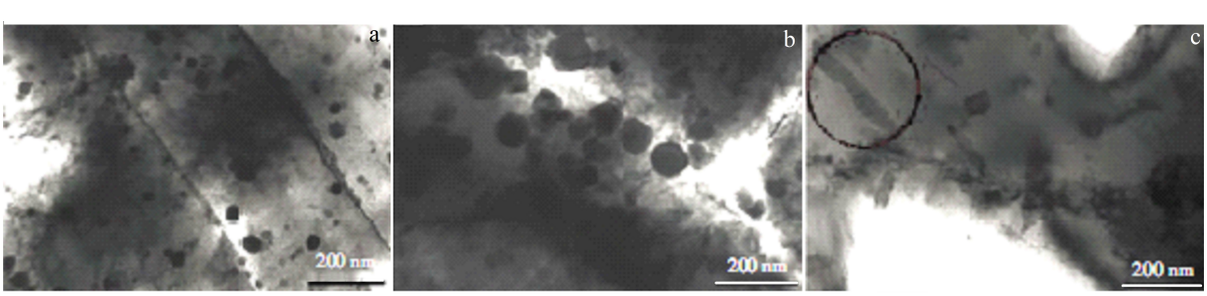

Fig.8 TEM images of second phase particles distribution of molybdenum alloys doped with different rare earth elements[7]: (a) Mo-0.1La, (b) Mo-0.1Y, and (c) Mo-0.1Ce

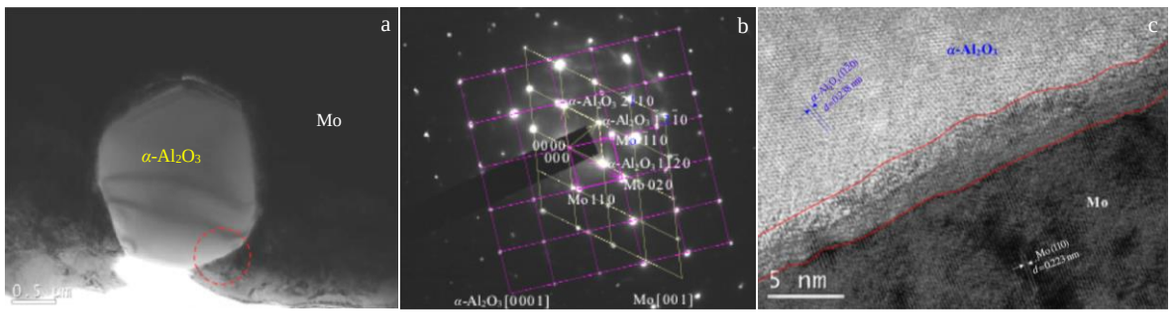

Fig.9 TEM images (a, c) and SAED pattern (b) of Mo-Al_2O_3 interface in sintered composite material: (a) Mo-Al_2O_3 combined state; (b) SAED pattern and (c) two-phase interface of red dotted circle in Fig.9a[35]

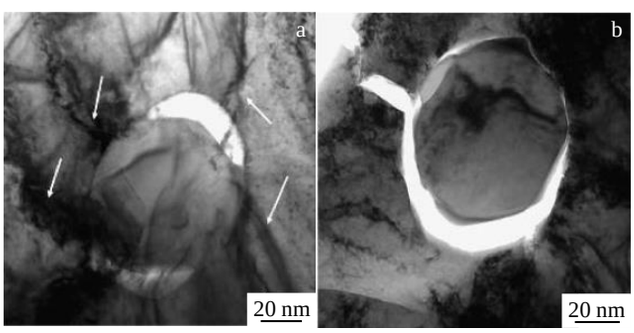

Fig.10 TEM images of Mo-1.5ZrO_2 alloy after compression test: (a) dislocation pile-up and (b) crack deflexion mechanism[39]

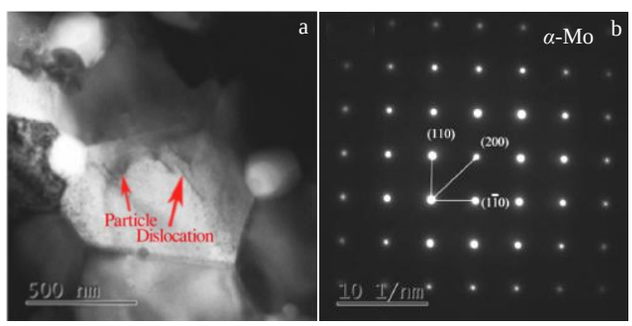

Fig.11 TEM image of dislocations in MSB-ZrB_2 alloy (a) and SAED pattern of Mo[42]

movement and results in the strengthening effect. In Fig.10b, the crack between the second phase and the matrix is formed and grow with the proliferation, slippage, and accumulation of dislocation during high temperature creep tests. TEM observation shows that crack extension is mainly controlled by the eutectics of intragranular structures with nanosized and micron ZrO_2 phases, resulting in the strong fracture process.

Mo-12Si-8.5B-ZrB_2 (MSB-ZrB_2) alloys were prepared by mechanical alloying followed by hot pressing[40-42]. Quantitative analyses indicate that both Hall-Petch and Orowan mechanisms play the significant role. The mechanical property improvement of fracture toughness and strength can be associated with the reduction of impurities derived from the reaction between ZrB_2 and impurity oxygen. The cohesion of grain and phase boundary is enhanced by Zr addition and the corresponding toughening and strengthening mechanisms are related to the ultra-fine grains and dispersed nanosized particles with tendency of interacting with moving dislocations and changing the distribution of dislocation, as shown in Fig.11.

In Fig.11, some isolated dislocations can be observed in the ductile α-Mo phase. These dislocations near the nanosized particles appear to be pinned, resulting in the dislocation accumulation inside the α-Mo grains. Therefore, these dispersed nanosized particles inside the grains decrease the stress concentration and pin the dislocation to increase the flow stress and promote dislocation multiplication and accumulation in the grain interior to enhance the strain hardening-related ductility, eventually resulting in the enhanced fracture toughness and high strength. Additionally, the dislocation grows within a certain length scale, and the stress concentration caused by dislocation multiplication appears to be less because of the refined grains. Fig.12 shows that dislocations form a growing wall by dislocation reaction and rearrangement, which potentially forms sub-boundaries to refine the grain size. The reduction of grain size can also improve mechanical strength by providing an increasing grain boundary area. Numerous grain boundaries result in the hindrance of dislocation motion and storing of dislocations, thereby effectively enhancing the strength.

In summary, the addition of rare earth oxide, alumina, or ZrO_2 has promising strengthening effect. Many nanometer oxide particles distributed in grains are strengthened by dispersion, dislocation is effectively pinned, and plasticity is improved. A small number of oxide particles distributed in grain boundaries are used to pin the grain boundaries, which inhibits the grain growth and ensures thermal stability.

3.3 Bubble-reinforced molybdenum alloys

Bubble strengthening mainly refers to strengthening mechanism occurring in the high-temperature Mo alloy doped with Si, Al, and K based on potassium bubble theory in the late 1970s. It relies on the solid solution strengthening and the

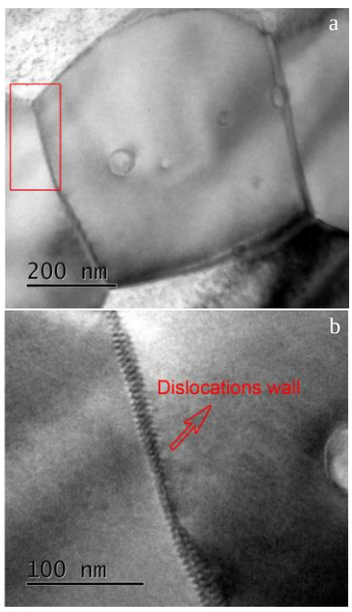

Fig.12 TEM images of MSB-ZrB_2 alloy: (a) subgrain and (b) dislocation of the rectangle area in Fig.12a[12]

formation of potassium bubbles at high temperature.

Some scholars believe that the strengthening phase of Al-Si-K (ASK) doped Mo wire not only shows pinning effect of potassium bubbles to hinder grain boundary migration, but also contains not completely decomposed dopant particles of potassium aluminosilicate. Therefore, the strengthening effect on the molybdenum wire includes the result of the joint action of K bubbles and the second phase dopant particles. During sintering process, the pinning effect of dislocations due to the formation of potassium bubbles can greatly reduce the mobility and moving speed of grain and subgrain boundaries. The second phase particles distributed in the grain boundary containing Si, Al, and K show dispersion strengthening. Therefore, the migration of the grain boundary is strongly pinned by the second phase particles, and the growth of the crystal grains can only proceed along a specific direction, leading to the formation of long grain structure for the dovetail-overlapped structure.

Therefore, the recrystallization temperature of the high-temperature Mo wire increases to 1800 °C, which is 400 °C higher than that of pure Mo wire. The grain structure after recrystallization is also changed from equiaxed crystal to grain structure with large length to width ratio. The mechanical properties, such as elongation and high temperature tensile strength, also significantly improve, as shown in Fig.13[43].

However, due to the short life cycle caused by the low melting points and vitalization property of Si, Al, and K, and the difficulty in composition control during doping and preparation processes, the application prospects of AKS alloy are restricted[44].

3.4 Composite reinforced molybdenum alloys

Among the various strengthening mechanisms of molybdenum alloys, the strengthening effect of trace elements is mainly effective at 1100~1300 °C, while the dispersion strengthening effect of carbides is the most obvious at 1400~1500 °C. At 1500~1800 °C, the rare earth oxide with high melting point has a strong strengthening effect while the carbide is soft and unstable. When the temperature is higher than 2000 °C, the rare earth oxide begins to soften, while the strengthening effect of doping of Si, Al, and K starts to dominate[32].

At present, the relatively mature composite toughening method for Mo alloy is combining the strengthening and toughening effects of addition of a large number of solid solution elements and carbides. Typical alloys are TZM, Zr-Hf-C-Mo (ZHM) -Y_2O_3, Mo-W-Hf-C and Mo-W-Hf-Zr-C alloys. For example, carbide-reinforced ZHM alloys after adding rare earth oxide Y_2O_3 can achieve an optimized property at medium to high temperature[45].

TZM alloy is prepared by adding Ti and Zr of no more than 1wt% in the Mo matrix. The solid solution strengthening is achieved by dissolving a small amount of Zr and Ti in the Mo matrix, while the second phase strengthening is achieved by the formation of fine carbide particles of Ti, Zr, and C in the matrix to prevent the dislocation movement[46]. In addition, TZM alloy can also undergo deformation strengthening below recrystallization temperature, and the distortion enhancement effect is increased with increasing the distortion. Zhang et al[19]

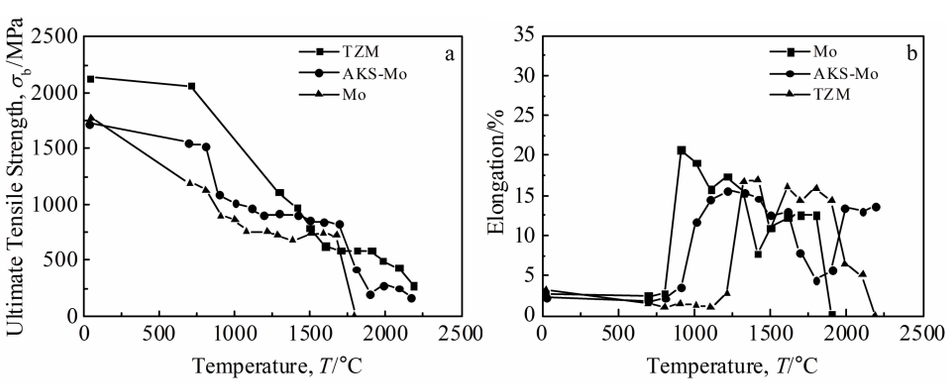

Fig.13 Ultimate tensile strength (a) and elongation (b) of Mo, AKS-Mo and TZM alloys[43]

reported the changes in the microstructure of the electron beam welded TZM alloy joints. A small amount of Zr and Ti was added into TZM alloy and few solid solution elements could be observed on Mo matrix, because most of them were combined with intracrystalline impurity element O to form oxides, such as ZrO_2 and TiO_2. The effect of solid solution strengthening depends on the size difference between solute and solvent atoms. The larger the size difference, the better the strengthening effect. Ref. [47] shows that the atomic sizes of Mo, Ti, and Zr are 2.8, 2.96, and 3.22 nm, respectively, so the solid solution strengthening effect of Zr and Mo is better. However, the industrial application of TZM alloys is restricted due to their poor oxidation resistance at high temperature and poor plastic toughness.

Yang et al[48] adopted PM route to prepare Mo-14wt% Re-1wt% La_2O_3 (ODS Mo-Re) alloys. The prepared alloys can be divided into stress relief annealing state, partially recrystallized state, and fully recrystallized state. The recrystallization initiation temperature is about 1300 °C, and the complete recrystallization temperature is about 1350 °C, which is about 200 °C higher than that of Mo-1wt% La_2O_3 alloy. The tensile strength at the complete recrystallization temperature increases by 50 MPa.

4 Conclusion and Prospect

Molybdenum and its alloys are indispensable materials with great application potential for the development of modern technology, but their performance needs to be further improved.

1) The brittleness of Mo is mainly caused by the characteristics of electronic distribution, the enrichment of interstitial impurities at the grain boundary, and the processing method. Since intrinsic brittleness can hardly be changed, the researches about optimized improvement of extrinsic brittleness and preparation process are the main directions.

2) On the basis of the existing powder metallurgy preparation process, the liquid-liquid mixing process significantly improves the uniformity and mechanical properties of the materials. The further development direction should be focused on improving the controlling measures of uniformity doping of the second phase, the dispersion of micro-region elements, and the uniformity of the distribution of gap elements between the second phase and the substation interface.

3) The developing of new preparation processes and providing materials with better structure and performance are the key developing directions and also a severe challenge. Research focus has changed currently from the single addition of alloying element, carbides, or oxides to multi-component composite doping, from single mechanism to multi-element comprehensive mechanism, from the improvement of strength and toughness to the controllable preparation of nano-scale second phase particles. However, the simultaneous optimization of the strength and toughness, oxidation resistance at high temperature, and the control of trace impurity elements have not been solved. The multi-component doping and comprehensive consideration of synergistic effects of combined strengthening mechanisms seem to be a feasible solution.

4) Further investigation of industrialized mass production method is urgent for realizing the quantity production and large-scale application of high-performance Mo alloys.

References

1 Wang Yi, Wang Dezhi, Sun Aokui *et al. Material Review*[J], 2012, 26(1): 137 (in Chinese)

2 Lang D, Pöhl C, Holec D *et al. Journal of Alloys and Compounds*[J], 2016, 654: 445

3 Tan Hui, Sun Qichun, Zhu Shengyu *et al. Tribology International* [J], 2020, 150: 106 344

4 Hu Ping, Yang Fan, Deng Jie *et al*. *Journal of Alloys and Compounds*[J], 2017, 711: 64

5 Hu Boliang, Wang Kuaishe, Hu Ping *et al. International Journal of Refractory Metals and Hard Materials*[J], 2020, 95: 105 439

6 Liu Gang, Zhang Guojun, Jiang Feng *et al. Materials China*[J], 2016, 35(3): 205 (in Chinese)

7 Fu Xiaojun. *China Tungsten Industry*[J], 2016, 31(3): 63 (in Chinese)

8 Zhang Yongyun, Wang Ting, Jiang Siyuan *et al. Materials Science and Engineering A*[J], 2017, 700: 512

9 Tan Wang, Chen Chang, Wang Mingpu *et al*. *Material Review* [J], 2007, 2l(8): 80 (in Chinese)

10 Han Qiang. *China Molybdenum Industry*[J], 2002, 26(4): 32 (in Chinese)

11 Zhang Yong, Wang Xiongyu, Yu Jing *et al. Material Review*[J], 2017, 31(7): 83 (in Chinese)

12 Tian Jiamin M, Liu Pinpin, Fan Jinglian *et al. China Tungsten Industry*[J], 2008, 8(4): 27 (in Chinese)

13 Yang Xiaoqing, He Yuehui, Luo Zhenzhong *et al. Rare Metals Letters*[J], 2006, 25(3): 30 (in Chinese)

14 Cheng P M, Zhang Z J, Zhang G J *et al. Materials Science and Engineering A*[J], 2017, 707: 295

15 Liu G, Zhang G J, Jiang G *et al. Nature Materials*[J], 2013, 12(4): 344

16 Kaserer L, Braun J, Stajkovic J *et al. International Journal of Refractory Metals and Hard Materials*[J], 2020, 93: 105 369

17 Eck R. *International Journal of Refractory & Hard Metals*[J], 1983, 2: 39

18 Fan Jinglian, Cheng Huizhao, Lu Mingyuan *et al. Rare Metals Materials and Engineering*[J], 2008, 37(8): 1471 (in Chinese)

19 Zhang Y Y, Wang T, Jiang S Y *et al. Materials Science and Engineering A*[J], 2017, 700: 512

20 Leichtfried G, Joachim H S, Martin H. *Metallurgical and Materials Transactions A*[J], 2006, 37(10): 2955

21 Sturm D, Heilmaier M, Schneibel J H *et al. Materials Science and Engineering A*[J], 2007, 463(1-2): 107

22 Ohser-Wiedemann R, Martin U, Müller A *et al. Journal of Alloys*

and Compounds[J], 2013, 560: 27
23 Wang Chengyang, Teng Yukuo, Dong Di *et al. Powder Metallurgy Technology*[J], 2018, 36(6): 418 (in Chinese)
24 Kitsunai Y, Kurishita H, Kuwabara T *et al. Journal of Nuclear Materials*[J], 2005, 346(2-3): 233
25 Kitsunai Y, Kurishita H, Narui M *et al. Journal of Nuclear Materials*[J], 1996, 239: 253
26 Kmishiha H, Asayama M, Tokunaga O *et al. Materials Transactions*[J], 1989, 30(12): 1009
27 Pöhl C, Lang D, Schatte J *et al. Journal of Alloys and Compounds*[J], 2013, 579: 422
28 Lang D, Povoden-Karadeniz E, Schatte J *et al*. *Journal of Alloys and Compounds*[J], 2017, 695: 372
29 Siller M, Lang D, Schatte J *et al. International Journal of Refractory Metals and Hard Materials*[J], 2018, 73: 199
30 Yang Lilin, Zhang Qifu, He Zhiyong *et al. Materials Science and Engineering of Powder Metallurgy*[J], 2018, 23(2): 137 (in Chinese)
31 Zhou W W, Sun X H, Kikuchi K *et al. Materials and Design*[J], 2018, 146: 116
32 Zhang G J, Sun Y J, Niu R M *et al. Rare Metal Materials and Engineering*[J], 2005, 34(12): 1926 (in Chinese)
33 Feng Pengfa, Fu Jinbo, Zhao Hu *et al. Metal Powder Report*[J], 2016, 71(6): 437
34 Hu Yajie, Xu Liujie, Zhou Yucheng *et al. Transactions of Materials and Heat Treatment*[J], 2015, 36(6): 15 (in Chinese)
35 Zhou Hang. *Preparation, Microstructure and Properties of Mo Matrix Composites Reinforced by Al_2O_3 Particles*[D]. Xi ' an: Xi'an University of Technology, 2015
36 Dai Baozhu, Zhong Shiwei, Xu Liujie *et al. Journal of Henan University of Science & Technology: Natural Science*[J], 2010, 31(1): 1 (in Chinese)
37 Xu Liujie, Wei Shizhong, Zhang Dandan *et al. International Journal of Refractory Metals and Hard Materials*[J], 2013, 41: 483
38 Fan Xiaoman, Xu Liujie, Wei Shizhong *et al. Ceramics International*[J], 2020, 46(8): 10 400
39 Cui Chaopeng, Zhu Xiangwei, Li Qiang *et al. Journal of Alloys and Compounds*[J], 2020, 829: 154 630
40 Wang Juan, Li Bin, Li Rui *et al. International Journal of Refractory Metals and Hard Materials*[J], 2020, 86: 105 129
41 Li Rui, Zhang Guojun, Li Bin *et al. International Journal of Refractory Metals and Hard Materials*[J], 2017, 68: 65
42 Wang Juan, Ren Shuai, Li Rui *et al. Progress in Natural Science: Materials International*[J], 2018, 28(3): 371
43 Zhang Hongbin, Zhu Yaomin, Zhao Shengli *et al. Hot Working Technology*[J], 2008, 37(22): 32 (in Chinese)
44 Wang Y, Gao J C, Chen G M *et al. International Journal of Refractory Metals and Hard Materials*[J], 2008, 26(1): 9
45 Yi Yongpeng. *China Molybdenum Industry*[J], 1995, 19(5): 42 (in Chinese)
46 Huang Qiang, Li Qing, Song Jinxia *et al. Materials Reports*[J], 2009, 23(21): 38 (in Chinese)
47 Ma Quanzhi. *China Molybdenum Industry*[J], 2012, 36(4): 41 (in Chinese)
48 Yang Yichao, Lin Xiaohui, Li Yanchao *et al. China Molybdenum Industry*[J], 2020, 44(3): 46 (in Chinese)

钼合金的强韧化研究现状及展望

王　苗[1,2]，杨双平[1]，刘海金[1]，杨　鑫[1]，王利东[1]
(1. 西安建筑科技大学 冶金工程学院，陕西 西安 710055)
(2. 陕西省冶金工程技术研究中心，陕西 西安 710055)

摘　要：钼及其合金以其诸多优异的性能在各个领域内受到广泛关注，但其抗蠕变性能、高温强度及抗氧化的劣化以及批量化生产手段的不足限制了大规模的工业应用。本文综述了金属钼的脆性来源，指出非本征脆性的改进及制备工艺的革新是钼合金研究和开发的重点方向。介绍了目前钼合金强韧化的主要形式，列举了典型钼合金研究开发现状，总结了钼合金的研究方向。

关键词：钼合金；强韧化；粉末冶金技术；固溶强化；第二相弥散强化；合金化

作者简介：王　苗，女，1984年生，博士，讲师，西安建筑科技大学冶金工程学院，陕西 西安 710055，电话：029-82202923，E-mail：wmxauat@163.com